ELSEVIER

Seminars in
NUCLEAR
MEDICINE

Radiomicrosphere Dosimetry: Principles and Current State of the Art

Seza A. Gulec, MD, FACS, FACNM and Anthony J. McGoron, PhD

Radiomicrosphere Therapy (RMT) refers to a liver-directed therapeutic modality based on the intrahepatic arterial administration of radiolabeled microspheres. There is a need for standardization of the terminology of RMT. A descriptive identifier should first name the radioisotope, then the chemical formulation of the microsphere, and lastly add the term RMT that indicates the therapeutic modality. At present, clinically available options include |*Y-90*| |*Resin*| |*RMT*|, |*Y-90*| |*Glass*| |*RMT*| *and* |*Ho-166*| |*PLLA*| |*RMT*|. The latter is available in Europe and is being considered for clearance by the FDA in the United States. Preclinical studies with |*Re-188*| |*PLLA*| |*RMT*| are underway. Dosimetric considerations are strongly tied to both the type of the radioisotope and the chemical composition of the microsphere type. This review will focus on Y-90 resin and glass RMT, the history, dosimetry, clinical use, and controversies.

Semin Nucl Med 52:215-228

The Namesake Dispute

Due to the lack of a standardized nomenclature, different names have been and are being used for RMT. The modality was first conceptualized and developed in the 1960s by Irvin Ariel, a New York surgeon with extensive scientific, and clinical involvement with nuclear medicine applications in his time.[1-5] The first radiomicrospheres for clinical application developed by Ariel was Yittrium-90 (Y-90) ceramic microspheres. The scientific and intellectual basis of the modality and its early clinical results were published by him in the 1970s.[6-9] Interestingly, the second radiomicrospheres, Y-90 resin, were also developed by a surgeon, Bruce Gray. Y-90 resin microspheres were the first RMT to receive FDA approval.[10,11] Gray's contributions to the science of RMT are colossal. The physiologic basis of the selective distribution of microspheres in liver tumors, the flow kinetics and patterns of microsphere distribution in normal liver and tumor tissue, and most importantly, the earliest dosimetric evaluations were all performed by Gray.[12-19] Gray named the modality selective internal radiation treatment (SIRT), associating the name to a company he founded. Despite extensive in-vivo dosimetric studies performed by Gray, his product was released with administered activity recommendations, but not with a formal dosimetric assessment requirement. The FDA approved the product in 2002 as a "medical device and/or brachytherapy device." The company pursued the medical device approval track with the FDA, which, at the time, did not require extensive phase 3 studies but demonstration of safety only. Every individual radioactive microsphere, in a vial containing millions of them, were considered brachytherapy implants and/or seeds. The package insert provides a formula to calculate the administered activity based on body surface area. Much of the clinical and dosimetric work during the early years of the use of the FDA approved Y-90 resin microspheres was performed by Andrew Kennedy, a radiation oncologist. Kennedy's work provided unique scientific contribution specific to the dosimetry of RMT, particularly from a radiation oncology perspective.[20-26] Kennedy introduced the term "microsphere brachytherapy" for the modality.[27] However, the term SIRT continued to dominate the literature, and the dosimetric work for RMT evolved in the medical internal radiation dosimetry (MIRD) track.

The FDA had given approval for humanitarian device examination for Y-90 glass microspheres in 1999 as brachytherapy device that was restricted for hepatocellular carcinoma (HCC) only. This particular radiomicrosphere was subjected to greater FDA scrutiny requiring a robust clinical trial of a phase 3 design, eventually receiving full approval.[28,29] Much of the early

Department of Surgical and Nuclear Oncology Research Florida International University Herbert Wertheim College of Medicine, Miami, FL.

Address reprint requests to Seza Gulec, MD, FACS, FACNM, Department of Surgical and Nuclear Oncology Research Florida International University Herbert Wertheim College of Medicine, Miami, FL E-mails: sezagulec@gmail.com, sgulec@fiu.edu

https://doi.org/10.1053/j.semnuclmed.2021.12.009
0001-2998/

work using these particular radiomicrospheres was performed by Riad Salem, an interventional radiologist. Salem coined the term "Y-90 radioembolization" simply due to the interventional radiology technical similarities with chemoembolization.[30,31] This term found popularity in the clinical community and acceptance in the literature. Salem's work provided significant contribution specific to the technical aspects of the modality as well as clinical treatment planning of RMT, particularly from an interventional radiology perspective.[32-36] The term later was modified to transarterial radioembolization (TARE) for a better rhyme with transarterial chemoembilization (TACE). Despite their popularity, radioembolization and transarterial readioembolization, in the strictest terms, are misnomers. The treatment is not an embolic treatment. An embolic treatment aims at cutting off the blood flow creating ischemia. Quite the contrary, maintenance of adequate O2 is required for an effective generation of reactive oxygen species (free radicals) for desired internal radiation effect. Transarterial administration merely voices the delivery route. Among oncologists, the RMT modality found a slang term "Y90 treatment." The majority of the clinical work in the world was performed using Y-90 resin or glass microspheres. The quest for an ideal radiomicrosphere for clinical use paralleled the expanding clinical applications of RMT.[37-41] We introduced and stand behind the term of "radiomicrosphere therapy" as the most appropriate term for this clinically sound treatment modality.[42-45] One can develop different microspheres with different chemical or physical properties, and any microsphere can be labeled with any beta particle emitting radioisotope. New radiomicrospheres are being evaluated and introduced into clinical use as the modality is establishing its role in the management of primary and metastatic liver cancers. Rhenium-186 poly lactic acid (PLA)[41] and Holmium-166 PLA (QuiremSphere) made it to clinical trials,[46] and the latter obtained approval in Europe in 2015.[47] The RADIOMICROSPHERE THERAPY term leaves behind all commercial and professional biases and best describes the nature of the modality.

The Intellectual and Scientific Basis of Y-90 RMT

The intellectual basis of Y-90 radiomicrosphere treatment is the preferential distribution of microspheres, yielding much higher concentrations in the tumor compartment than the normal liver parenchyma, when injected into the hepatic

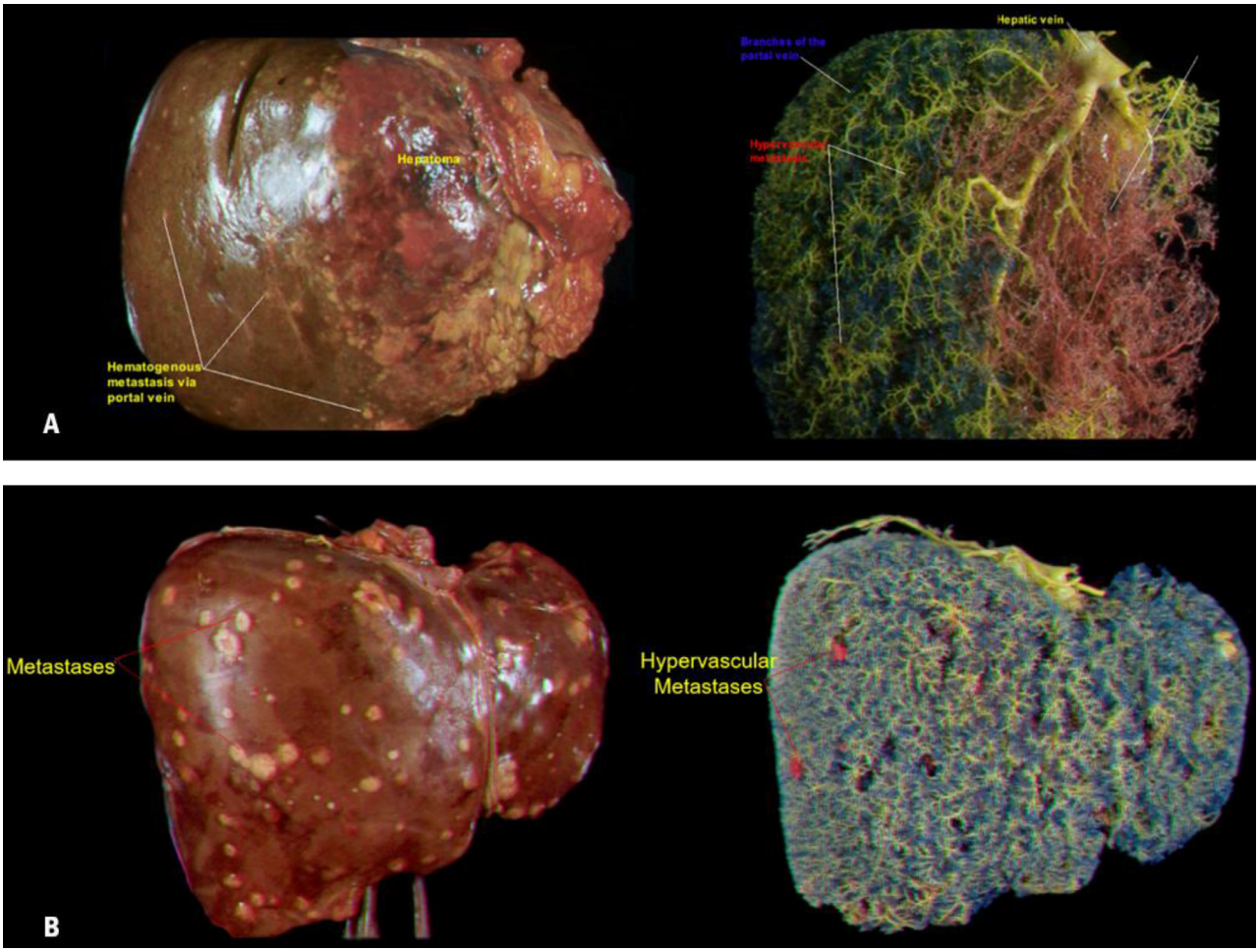

Figure 1 (A, left) Picture of a liver containing a large hepatoma as well as small hematogenous metastatses deposited through the portal vein and (A, right) a cast displaying the vascular architecture. (B, left) A picture of a liver with multiple small metastases and (B, right) visual demonstration of hypervascular metastases.

artery. This selectivity is due to the fact that the tumor blood supply is overwhelmingly derived from the hepatic artery, since the neo-vasculature of angiogenesis is rooted from the hepatic artery branches, while normal liver blood supply is about 75% from the portal vein (Fig. 1). Tumor angiogenic development starts when the tumor reaches an approximate size of 1mm. However, an adequate tumor to normal liver blood flow differential is not established to produce a favorable therapeutic profile (risk-benefit ratio) with RMT. Thus, there is no role for RMT for micrometastatic disease or small-volume macrometastatic disease. Conversely, after exceeding a threshold volume, due to central necrosis, microsphere delivery is hindered. The therapeutic profile, once again, is compromised.

The Governing Physics and Dynamics of Y-90 RMT

Yittrium-90 (Y-90) is a high energy beta particle radiating radioisotope with a physical half-life of 64.2 hours (2.67 days) (Fig. 2). It is incorporated in biocompatible microspheres measuring 30-40 microns. Intrahepatic arterially administered Y-90 microspheres are entrapped in the microvasculature, and release beta radiation (energy maximum, 2.27 MeV; mean, 0.9367 MeV) with an average penetration range of 2.5 mm and a maximum range of 11 mm in tissue (Fig. 3). In therapeutic use, 94% of the radiation is delivered over 11 days. The high tumor to liver concentration ratio of Y-90 radiomicrospheres results in an effective tumoricidal radiation absorbed dose whilst limiting the radiation injury to the normal liver.

Both the resin microspheres (SIR-Spheres; Sirtex Medical, Sydney, Australia) and the glass microspheres (Thera-Sphere; MDS Nordion, Ottawa, Ontario, Canada) have relatively consistent size ranging from 20-40 microns, and neither is

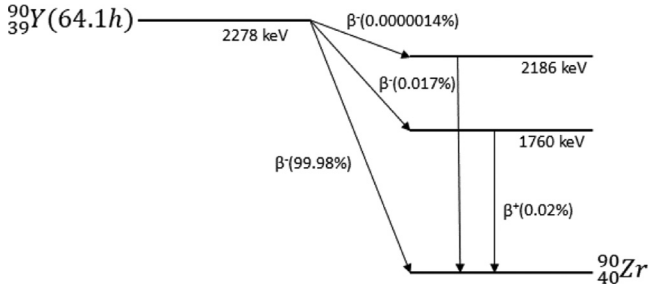

Figure 2 Decay scheme of Y-90.

metabolized or excreted but remain in the liver permanently. The absence of biological clearance of microspheres simplifies dosimetry compared to other radiopharmaceutical therapies. The main differences between the resin and glass radiomicrospheres are in the density (g/cc) and specific activity (activity per sphere). The glass radiomicrospheres are 3 times heavier per volume, and carry 50 times more activity per weight than resin radiomicrospheres (Table 1).

Microspheres are injected into the branches of the hepatic artery using a microcatheter. The size, weight and density (number of microspheres per given volume) of radiomicrospheres and their flow impedance in the microcatheter affect the delivery kinetics.[48-50] The fractal branching of the hepatic artery is not symmetrical and the microvascular anatomy of the tumors is irregular leading to an inherent non−uniformity in microsphere deposition. All these factors together result in an inhomogeneous dose distribution and consequently complicate dosimetry and predictions of the therapeutic outcome.

The desired size and number of the microspheres for the most uniform distribution with optimal tumor to liver ratio were tested in preclinical studies performed by Gray et al.[14] The vascular supply of liver tumors were extensively studied by Ackerman et al.[51-58] Capillaries within rapidly growing tumors are much larger than normal, appearing as sinusoid-

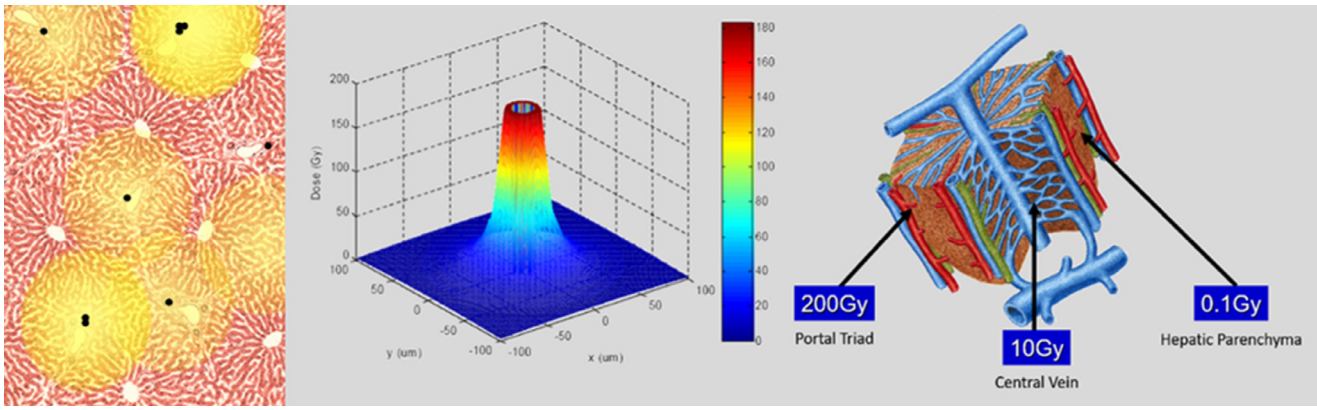

Figure 3 (Left) Graphic of single or clumps of microspheres deposited in the lobules of the liver. (Center) Radial dose profile around 32-mm-diameter Y-90 microsphere (50-Bq initial activity) that extends to 1 cm. (Right) Hepatic lobular architecture of the central vein which runs along central the axis of each lobule, all of which merge to form hepatic veins. Hepatocytes occupy the greatest volume of a lobule, forming cords between portal triads, and central vein, separated by sinusoids. Microsperes lodge in the portal triad arterioles located at the hexagonal corners.

Table 1 Comparison of the Y-90 Microspheres Approved for Clinical use

	SIR-Spheres	Thera-Spheres	Quirem Sphere
Isotope	Y-90	Y-90	Ho-166
Material	Resin	Glass	poly(L-lactic acid)
Loading	Absorbed	Embedded	Embedded
Size	20-60 μm (<10% smaller than 30 or > 35 μm)	20-30 μm	16-60 μm (97% between 15 and 60 μm)
Density	1.1 g/cc	3.3 g/cc	1.4 g/cc
Activity	3 GBq	From 3 to 20 GBq	240-375 Bq/microsphere
Volume	5 cc in water	0.6 cc water	Patient specific
# of spheres	40-80 M	22-73 k	Patient specific
Approved indications	Metastatic colorectal liver cancer	Hepatocellular Carcinoma (HCC)	Unresectable liver tumors
Loading	Y-90 absorption post-microsphere synthesis	Inactive Y-89 embedded in glass neutron activation to Y-90	Inactive 165-Mo embedded into the polymer neutron activation of 165-Ho
Year approved	2002 (FDA)	2021 (FDA)	2015 (EMA)

like vessels with little tendency to differentiate into arterioles and venules. The dimensions of new vessels in a Walker 256 carcinoma were found to range from 25 to 75 μm in diameter; compared to normal capillaries of ~5 μm and arterioles 2-30 μm in diameter. It may be expected that the pattern of distribution of intra-arterially administered microspheres in the liver and tumor varies with microsphere size as well as the anatomy of the tumor microvasculature.

Dosimetry

Dosimetry Primer and Medical Internal Radiation Dosimetry Formalism

Dosimetry is defined as the determination of the radiation absorbed dose ($\dot{D}$) in target tissues from a given administered activity (A_0). Absorbed dose ($\dot{D}$) is dependent on the cumulated activity ($\tilde{A}$). Cumulated activity ($\tilde{A}$) is the total amount of activity built over the time the radioactivity resides in the target. Though the main component is the beta particle radiation, the cumulated activity ($\tilde{A}$) includes all photon and particle emissions resulting from the process of decay and mathematically calculated as the area under the time-activity curve (Figure 4a). Radiation deposition occurs in a defined volume, and geometry and is dependent on the absorption characteristics of the particular tissue. The physical determinants of radiation deposition are expressed under a single calculable appraise called the "S-value." The central dogma for the absorbed dose in medical internal radiation dosimetry (MIRD) formalism is that the absorbed dose is the product of cumulated activity and the "S-value."

The simplified mathematical formulation of this concept is given by:

$$\dot{D} = \tilde{A}\ X\ S$$

The core mathematical expression of this concept is given by:

$$\dot{D}(r_T, t) = \sum_{r_s} A(r_S, t) * S(r_T \leftarrow r_S, t)$$

$A(r_S, t)$: Time-dependent activity of the radiopharmaceutical in source tissue r_S

$S(r_T \leftarrow r_S, t)$: The radionuclide-specific quantity representing the mean absorbed dose rate to target tissue r_T at time t after administration per unit activity present in source tissue r_S

The core mathematical expression for "S-value" is:

$$S(r_T \leftarrow r_S, t) = \frac{1}{M(r_T, t)} \sum_i E_i Y_i * \phi(r_T \leftarrow r_S E_i, t)$$

$$= \frac{1}{M(r_T, t)} \sum_i \Delta_i * \phi(r_T \leftarrow r_S E_i, t)$$

E_i: Mean (or individual) energy of the i^{th} nuclear transition

Y_i: Number of i^{th} nuclear transitions per nuclear transformation

Δ_i: The product of E_i and Y_i (mean energy of the i^{th} transition per nuclear transformation)

ϕ ($r_T \leftarrow r_S$, E_i, t): Absorbed fraction (defined as the fraction of radiation energy E_i emitted within the source tissue r_S at time t that is absorbed in the target tissue r_T) (~ 1 for beta particles)

$M(r_T, t)$: Time-dependent mass of the target tissue r_T in the reference individual

The quantity S is specific to: (1) radionuclide (2) the tissue compositions of r_S and r_T (3) the computational phantom defining the spatial relationship (volume and geometry) between radiation and organ(s). Organ geometries, volumes, and location are typically defined by standard anthropomorphic phantoms (Fig. 4b). D = $\tilde{A}$ × S, where $\tilde{A}$ (cumulated activity) is the area under the curve (Figure 4a).

Clinical Dosimetry

A clinical dosimetry is defined as a method of calculation of absorbed dose in the target tumor tissue and the organs and/or tissues at risk during RMT utilizing imaging tools to measure the relative distribution of radioactivity. Dosimetry can be performed prior to or after the RMT. A post-treatment dosimetry can be performed utilizing the bremsstrahlung radiation or the positron emissions from the decay of the Y-90 (Fig. 2). The post-treatment dosimetry has no theranostic value, as by

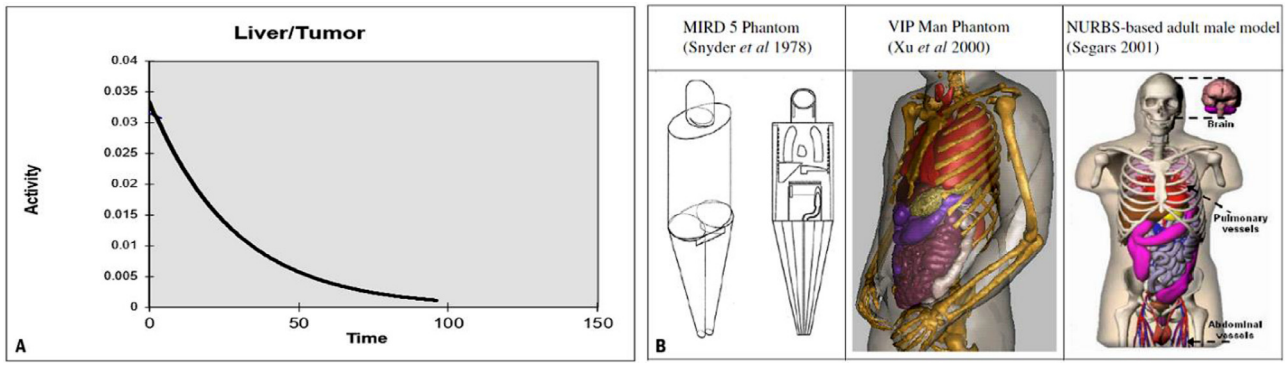

Figure 4 A: Time − Activity curve for radiomicrospheres. Cumulated activity is the area under the curve ($\widetilde{A}$). For non-degradable microspheres it follows the physical decay scheme. B: Comparison of the realism of the traditional MIRD body antrophomorphic models where the "S-value" derived for modelling.[59]

definition, it is post-facto. However, the dose-response relationship can be realistically, but not necessarily most accurately, determined in the post-treatment setting. The potential accuracy of post-RMT dosimetry is attenuated due to the difficulty in obtaining high quality images with bremsstrahlung or the positron emissions. A post-treatment dosimetry is confirmatory in nature. The data simply validates the tumor absorbed dose and objective response relationship.

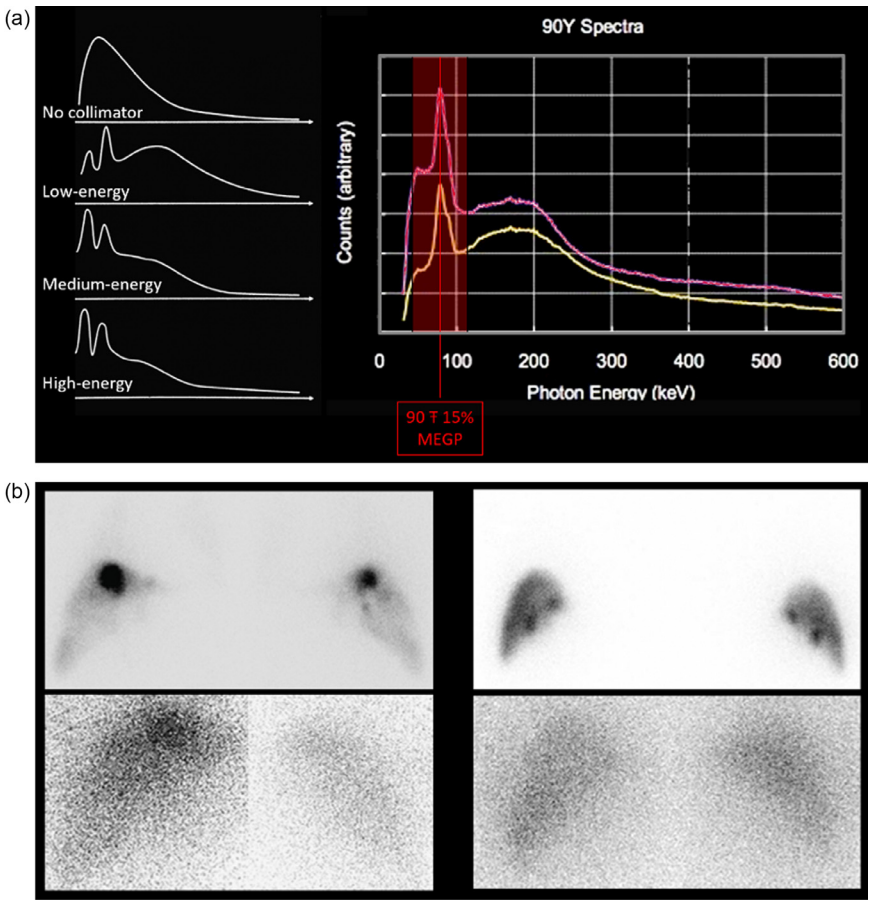

Figure 5 a: Photon spectra of Y-90 bremsstrahlung radiation and example of windowing possibilities for SPECT imaging. b: (top) Tc-99m MAA SPECT imaging of liver tumors prior to RMT. (bottom) Y-90 bremsstrahlung of the same liver tumors post RMT.

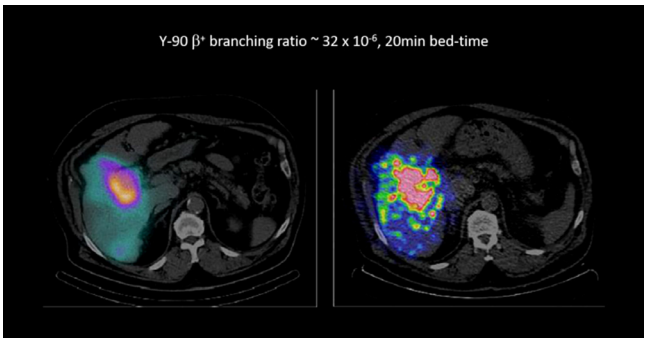

Figure 6 (Top) Tc-99m MAA SPECT imaging of liver tumors prior to RMT. (Bottom) Y-90 bremsstrahlung of the same liver tumors post RMT.

Post-treatment Bremsstrahlung Imaging and Dosimetry

Bremsstrahlung ("braking radiation" or "deceleration radiation") is electromagnetic radiation produced by the deceleration of a charged particle when deflected by another charged particle, typically deceleration of an electron by an atomic nucleus. The moving particle loses kinetic energy, which is converted into an X-ray photon. Bremsstrahlung has a continuous spectrum (Fig. 5a), which degrades image quality, and quantitation accuracy. SPECT imaging has clear advantages over planar imaging for Bremsstrahlung quantitation. The poor image quality of Bremsstrahlung compared to Tc-99m gamma imaging is illustrated in (Figure 5b). Several protocols have been suggested to optimize the image quality and quantitative power of bremsstrahlung imaging.[60-66]

Post-treatment PET/CT Imaging and Dosimetry

Y-90 has 0.02% positron emission (see Fig. 2). This has been utilized in obtaining post-treatment PET/CT images (Fig. 6). The low emission rate prolongs image acquisition time. Obtaining a familiar clear PET image is possible, but would take unacceptably long imaging time. Multiple publications claim that a reasonable compromise can be attained between image quality with quantitative power and acquisition time that would not be prohibitive to clinical flow.[67-70]

Pre-treatment Prescribed Activity

The "prescribed activity" is suggested for Y-90 resin RMT. It is essentially based on liver volume-activity distribution projections based on body surface area (BSA). It is based on the supposition that the BSA correlates with liver volume in the normal population. It is not a true dosimetry methodology. The calculation of the prescribed activity is provided to serve as a reference. The recommended method for calculating the administered activity for an individual patient with SIR-Spheres is the Body Surface Area (BSA) method.

$$\mathrm{BSA} = 0.20247 * \mathrm{H}^{0.725} * \mathrm{W}^{0.425}$$

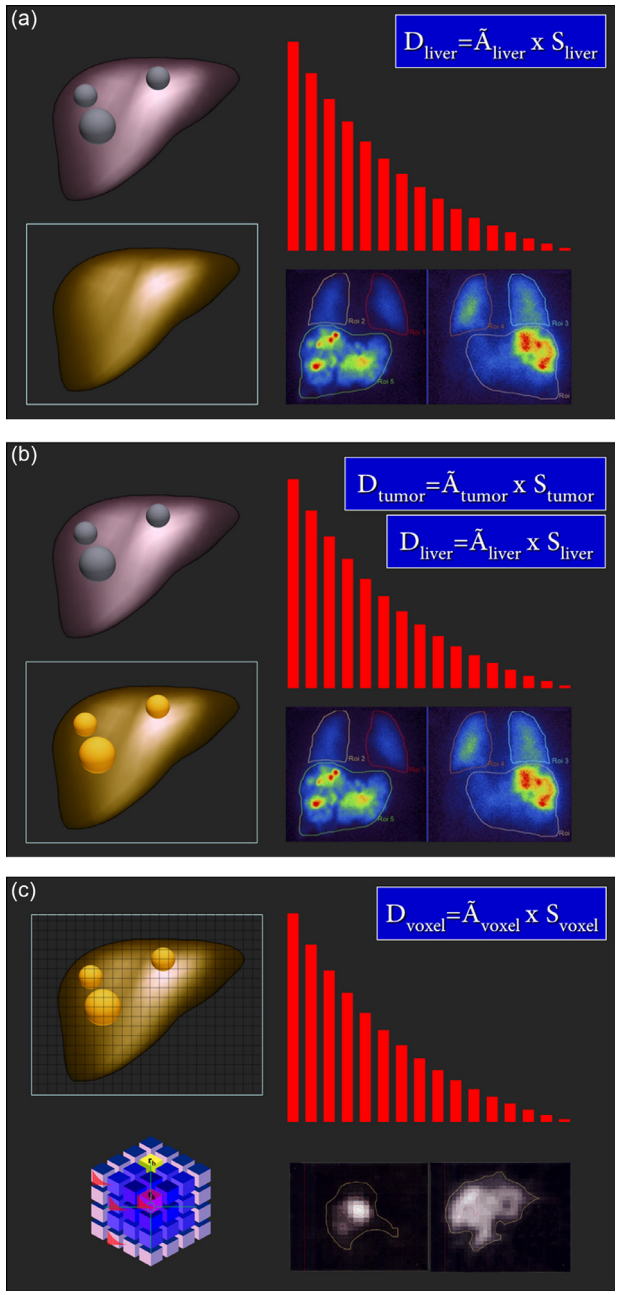

Figure 7 Graphical representation of Dosimetry Methods. a: MIRD, Non-compartmental Dosimetry, b: MIRD, Compartmental Dosimetry (Partition Model), c: Voxel Dosimetry.

Prescribed activity calculation for whole liver and/or bilobar treatment

$$\text{Prescriberd Activity(GBq)} = (\mathrm{BSA} - 0.2) + \left(\frac{\mathrm{V_{tumor}}}{\mathrm{V_{tumor}} + \mathrm{V_{normal\ liver}}}\right)$$

Where:

V_{tumor} is the total volume of tumor in the liver

V_{normal} liver is the total volume of non−tumor liver tissue

Prescribed activity calculation fotr lobar or super-selective treatment

$$\text{Prescribed Activity(GBq)} = \left[\text{BSA} - 0.2 + \left\{\frac{\text{Tumor volume}_L}{\text{Total volume}_L}\right\}\right] * \left[\frac{\text{total volume}_L}{\text{Total liver volume}}\right]$$

Where:

Activity$_L$ is the prescribed activity for the lobe

Tumor volume$_L$ is the volume of tumor present in the lobe

Total volume$_L$ is the total volume of the lobe including the tumor in the lobe.

Total liver volume is the total volume of the liver including the tumor.

Pre-treatment Theranostic RMT Dosimetry

In contrast to post-treatment RMT dosimetry, pre-treatment dosimetry has a potential theranostic value. The RMT theranostic dosimetry is constructed upon reasonably accurate image-based data and a number of assumptions involving the rheology and intrahepatic distribution kinetics of the microspheres. There are 3 levels of clinical MIRD dosimetry that can be performed (1) MIRD, Non−compartmental (2) MIRD, Compartmental (also known as "the partition model") (3) MIRD, Voxel dosimetry.

MIRD, Non−compartmental Method

This is the most simplistic dosimetric method (Fig. 7a). The primary assumption is the even distribution of radiomicrospheres in the tumor and normal liver compartments, thus, it does not require surrogate imaging to differentiate the 2 compartments, and their relative vascular flow. Both the glass and resin microspheres are nondegradable, as such, there is no biologic elimination. The cumulated activity calculation is straightforward. The administered activity is known and the area under the time activity curve (Cumulated activity, $\widetilde{A}$) is a function of physical decay only.

This methodology was suggested for Y-90 glass microsphere RMT. The safe hepatic radiation absorbed dose figures provided in the early literature were all obtained using this method. There is some level of clinically acceptable safety parameters and information established by this method for hepatic toxicity.

The recommended method for calculating the administered activity for an individual patient using MIRD non−compartmental method uses the following measurement and calculations.

$$\text{Activity Required(GBq)} = \frac{[\text{Desired Dose(Gy)}] * [\text{Liver Mass (kg)}]}{50}$$

The liver volume and corresponding liver mass may be determined using CT or ultrasound.

$$\text{Liver Dose(Gy)} = \frac{50[\text{Injected Activity(GBq)}][1 - \text{F}]}{\text{Liver Mass(kg)}}$$

Where F is the fraction of injected radioactivity localizing in the lungs, as measured by Tc-99m MAA scintigraphy. The upper limit of injected activity shunted to the lungs is F X $A = 0.61$ GBq where F is the lung shunt fraction and A is the total activity injected.

Lung shunt fraction (following Tc-99m-MAA injection into the hepatic artery):

$$\%\ \text{shunt} = \left(\frac{\text{Lung counts}}{\text{Liver counts} + \text{Lung counts}}\right) * 100$$

Limiting the radiation exposure to ≤ 30 Gy is required.

Activity that may potentially reach the lung

$$A_{\text{lung(GBq)}=A_{\text{total}}*L/100}$$

Where: A_{lung} = lung activity (GBq); A_{total} = total prescribed activity (GBq); L = lung shunt (%)

The resulting lung dose, given that a given amount of activity shunts from the liver to the lung:

$$D_{\text{lung}}(\text{Gy}) = \frac{49670 * A_{\text{lung}}}{M_{\text{lung}}}$$

Where: D_{lung} = lung dose (Gy), A_{lung} = lung activity (GBq), M_{lung} = mass of the lung (Kg)

MIRD, Compartmental Method (Partition Method)

This method recognizes the inadequacy of the non−compartmental method and is based on the definition of tumor and normal liver compartments and the quantitation of respective blood flows in each compartment (Fig. 7b).

For Y-90 resin or glass microspheres this task requires a surrogate blood flow and/or distribution agent. This agent has been and is Tc-99m-macroaggregate albumin (MAA). Macroaggregate albumin (MAA) is a particulate form of albumin with an average size of 20-40 micron (with none greater than 150 micron.[71]). The recommended number of particles per injection is 200K-700K, with suggested number being 350K. Depending on the activity added to the vial, the volume varies from 0.2 to 2.0 mL. The density of MAA is close to that of resin microspheres but much lower than glass microspheres. The primary assumption with MAA is the "reasonable" representative distribution as a surrogate flow agent for the Y-90 microspheres. A formal MIRD formulation, taking into account tumor and liver compartments, was first proposed by Ho et al. in 1996[72]. This approach, at that time, was termed the "partition model." The original study was performed on 14 patients with hepatocellular carcinoma (HCC) and 3 patients with colorectal cancer liver metastases (CRCLM) using Y-90 Resin Microspheres. The validity of the model was verified by intraoperative dosimetry using a beta probe. The investigators reported a good correlation between the dose estimates using the partition model and

intraoperative dosimetry.[72] Further clinical validation study was reported by the same group in 1997 on a total of 95 patients treated with Y-90 resin microspheres using different administration techniques including open surgery, via hepatic arterial port infusion, and angiographic technique.[73] The study demonstrated that a dose considered to be tumoricidal was >120Gy. This study also concluded that an estimated dose of 30Gy to the lungs from a single treatment, using the partition model, could be considered safe. The MIRD, compartmental method assumes intra-compartmental distribution of MAA and the microspheres to be homogenous. The shape of MAA, in reality, is not spherical (Fig. 8), and therefore assuming a distribution the same as the radiomicrospheres is not strictly valid.

Tc-99m MAA is injected via the hepatic arterial catheter at the completion of the visceral angiography. Tc-99m MAA imaging was originally suggested for determination of lung shunt fraction (LSF), and identification of a possible extrahepatic gastrointestinal (GI) activity resulting from hepatofugal reflux, as part of safety assessment for resin microspheres. The LSF is determined using a geometric method on planar imaging. Available safety data is based on planar imaging. SPECT imaging has clear advantages over planar imaging as a quantitative modality in general. However, there is high level of clinically acceptable safety data established using planar imaging for evaluation, and prevention of lung toxicity. The MIRD Compartmental method has 3 shortcomings. (1) MAA is far from being a good surrogate flow agent. The sizes of the aggregates are not uniform (Fig. 8), they are subjected to additional clumping and or dissolution with free Tc-99m release. (2) The clear distinction of tumor and liver compartments may be challenging, more so with metastatic liver tumors due to the multiplicity of the tumors and the irregular pattern of disease distribution. This is more manageable with solitary large HCC lesions. Tomographic imaging offers better spatial resolution than planar imaging, yet, is inadequate to reflect inter, and intra compartmental variations in flow distribution. The tumor to liver ratio (TLR) index used in calculations for assessment of differential flow between respective compartments is imprecise. The commercially available MAA particles have been successfully labeled with Ga-68 for PET/CT which may potentially improve the quantitation capability.[74,75] A number of techniques have been reported and/or suggested to improve liver and tumor segmentation to optimize quantitative evaluation.[76-78] 3) The organ "S-values" have been tabulated based on computations using standard anthropomorphic phantoms (MIRD pamphlet 11).[79,80] Tumor involved liver can no longer be represented by a standard phantom. Furthermore, the "S-value" for irregular shape and size tumors is extremely problematic. "S-values" for tumors are approximated to a spherical volume, whereas, tumor geometry is incomparably more complex than a sphere. MIRD, compartmental dosimetry method may be improved by development of a better surrogate flow agent, preferably a PET agent. Development of radiomicrospheres with intrinsic theranostic power may be a superior solution. Examples for such radiomicrospheres includes Ho-166 PLLA and Re-188 PLLA.[40,41,81-83]

The dosimetric calculations for MIRD compartmental model are derived from the convictions explained below. Y-90 radiomicrospheres are distributed in the liver parenchyma with a concentration of C mCi/g. Because 1 mCi produces 3.7×10^4 disintegrations per second, energy released and absorbed per gram of tissue in 1s is 3.7×10^4 E_β MeV, where E_β is the average β-particle energy per disintegration, in mega−electron volts. The average β-particle energy per disintegration for Y-90 is 0.93 MeV. One rad is defined as 100 erg/g of tissue. It is equivalent to the absorption of 6.24×10^7 MeV/g:

$$\text{dose}_\beta\left(\frac{\text{rad}}{\text{s}}\right) = \frac{3.7 \times 10^4\left(\frac{\text{d}}{\text{s}}\right) \times \overline{\text{E}}_\beta\left(\frac{\text{MeV}}{\text{d}}\right) \times \text{C}\left(\frac{\mu\text{Ci}}{\text{g}}\right)}{6.24 \times 10^7\left(\frac{\text{MeV/g}}{\text{rad}}\right)}$$

$$= \text{C} \times \overline{\text{E}}_\beta \times 5.92 \times 10^{-4}\left(\frac{\text{rad}}{\text{s}}\right)$$

The average half-life is used to determine the total dose received during treatment and is equal to the half-life multiplied by 1.44. The half-life for Y-90 is 2.66 d. Therefore, the total dose for complete decay of Y-90 is

$$\text{dose}_\beta(\text{rad}) = \text{C} \times 0.9348 \times 51.2\left(\frac{\text{rad}}{\text{day}}\right) \times 2.66(\text{days}) \times 1.44$$

$$= \text{C} \times 184(\text{rad})$$

The administered Y-90 radiomicrosphere activity is distributed in tumor and normal liver compartments. The distribution profile is determined by the relative vascularity and volume of these 2 compartments and is expressed as the tumor-to-liver ratio (TLR). When lung shunting due to intrahepatic peritumoral arteriovenous communications occurs, a third compartment (lung) is encountered and is expressed as the lung shunt fraction (LSF). The TLR and LSF can be determined using Tc-99m macroaggregated albumin scans. Region-of-interest analysis of tumor and normal liver compartments on SPECT images is used to determine the TLR. The LSF is calculated on planar images using the formula below:

$$\text{LSF} = \frac{\text{counts}_{\text{lung}}}{\text{counts}_{\text{lung}} + \text{counts}_{\text{liver}}}$$

It is assumed that the administered activity is distributed evenly within the normal liver and tumor compartments. The tumor compartment, as expected, receives a higher concentration proportional to the TLR. Using the tumor and liver masses, the dose fraction accumulated in the normal liver (fractional liver uptake) is

$$\text{Fractional uptake}_{\text{liver}} = (1 - \text{LSF})\left[\frac{\text{Mass}_{\text{liver}}(\text{g})}{[\text{Mass}_{\text{tumor}}(\text{g}) \times \text{TLR}] + \text{Mass}_{\text{liver}}(\text{g})}\right]$$

The activity to be administered for a desired liver dose can be calculated as:

$$\text{activity}_{\text{admin}}(\text{mCi}) = \frac{\text{dose}_{\text{liver}}(\text{rad}) \times \text{m}_{\text{liver}}(\text{g})}{184,000 \times \text{fractional uptake}_{\text{liver}}}$$

$$\text{dose}_{\text{liver}}(\text{rad}) = \frac{\text{dose}_{\text{liver}}(\text{rad}) \times \text{m}_{\text{liver}}(\text{g})}{184,000 \times \text{fractional uptake}_{\text{liver}}}$$

Fractional tumor uptake (The fraction of the administered activity accumulated in the tumor) is

$$\text{Fractional uptake}_{\text{tumor}} = (1 - \text{LSF})\left[\frac{\text{TLR} \times \text{Mass}_{\text{tumor}}(\text{g})}{(\text{TLR} \times \text{mass}_{\text{tumor}}(\text{g})) + \text{mass}_{\text{liver}}(\text{g})}\right]$$

The doses to the tumor and lungs can be determined using the following equations

$$\text{dose}_{\text{tumor}}(\text{rad}) = \frac{\text{activity}_{\text{admin}}(\text{mCi}) \times 184,000 \times \text{fractional uptake}_{\text{tumor}}}{\text{m}_{\text{tumor}}(\text{g})}$$

$$\text{dose}_{\text{lung}}(\text{rad}) = \frac{\text{activity}_{\text{admin}}(\text{mCi}) \times 184,000 \times \text{SF}}{\text{m}_{\text{lung}}(\text{g})}$$

These formulas can be built into an Excel spreadsheet for clinical execution. A very practical smart phone application for quick calculations of activity to be prescribed using body surface area (BSA), MIRD non−compartmental and compartmental methods has been introduced by David Liu, a Vascular & Interventional Radiologist. Dosimetry and Activity Visualizer for Yttium-90 Radioembolization (DAVYR) is a smart phone application based on mathematical modelling built on acceptable assumptions and limitations. The application is meant as a general guide, and not intended for clinical use.

MIRD, Voxel Dosimetry Method

This method is the highest level of methodology applicable to clinical dosimetry. Voxel dosimetry can be defined as the calculation of radiation absorbed dose at the single voxel level. Activity determination is performed for every voxel in the image field. This is possible only with tomographic imaging. The cumulative activity is also defined at the voxel level, derived from patient specific SPECT or PET image data. At the voxel level, the volume, and geometry are constant. The voxels in different coordinates in a given volume may be exposed to different energy accretion, but this is known, and computable. Highly accurate "S-values" can then be determined for different voxel dimensions and radionuclides using direct Monte Carlo radiation transport simulations (Fig. 7c). In fact, the voxel "S values" are tabulated for a limited number of radionuclides including Y-90 (MIRD pamphlet 17[84]).

MIRD voxel dosimetry requires special software to implement. A number of software platforms are commercially available. These platforms and/or programs perform multiple post-image acquisition processing tasks and generate a clinically versatile output. Shared by most software platform functions are automated target and normal volume generation for improved accuracy, deformable image registration, time activity curve fitting and integration, 3D dosimetric evaluation functions for metrics such as dose-volume histogram and isodose displays, assessment and tracking of therapeutic response, functions for pretreatment and posttreatment workflows. Advanced dosimetric software platforms are being developed. Despite the highly sophisticated image processing capabilities and technical validation of their ex-vivo performance for activity and/or concentration determination, these platforms are not approved by the FDA Richetta for theranostic dosimetry. The FDA concern is linked to MAA not being a faithful surrogate for microsphere distribution.

Non−clinical, Computational Microdosimetry

Hepatic lobular, cellular, and subcellular dosimetric models exist. These mathematical model-based dosimetry techniques demonstrate the complexity of radiobiology, explain mechanisms of RMT-associated liver injury but do not generate patient-specific theranostic information.

Within the normal liver parenchyma, the microsphere distribution is confined to the portal tracts. Because of this unique localization pattern of the microspheres, even though the maximum range of β-particles in the liver is approximately 11 mm (5-10 times the lobule width), a significant fraction of absorbed dose is delivered within the portal tract domain. This dose absorption pattern explains the difference between external beam radiation- associated radiation-induced liver disease (RILD) and RMT-associated radiomicrosphere-induced liver disease (RMILD), in favor of the latter. Radial dose function analysis and spheric Monte Carlo modeling demonstrated a rapid fall in the absorbed dose within a short distance from the microsphere in a lobular lattice geometry (Fig. 3).[85] This model provides an essential dosimetric view as to the restricted radiation injury associated with RMT.[85]

Reported Safe Absorbed Dose Estimates in Y-90 RMT

The clinical objectives of dosimetry are to determine the administered activity that will deliver safe and effective radiation absorbed dose. Safety is defined as non−toxicity to the organs at risk, and efficacy is defined as achieving tumoricidal dose with RMT. Because RMT is a liver-directed therapy, the primary organ and/or target at risk is liver, and the primary safety criteria is the maximum tolerated dose (MTD) avoiding RMILD. The second organ and/or target at risk is the lung, as there is always a possibility of hepato-pulmonary microsphere shunting due to intra-tumoral arterio-venous malformations. Rarely, extrahepatic, and extrapulmonary toxicity may be encountered via specific complications. Radiomicrosphere reflux into the GI tract via hepato-fugal flow is possible. This is infrequent and preventable with a careful and skilled administration technique. Bone marrow

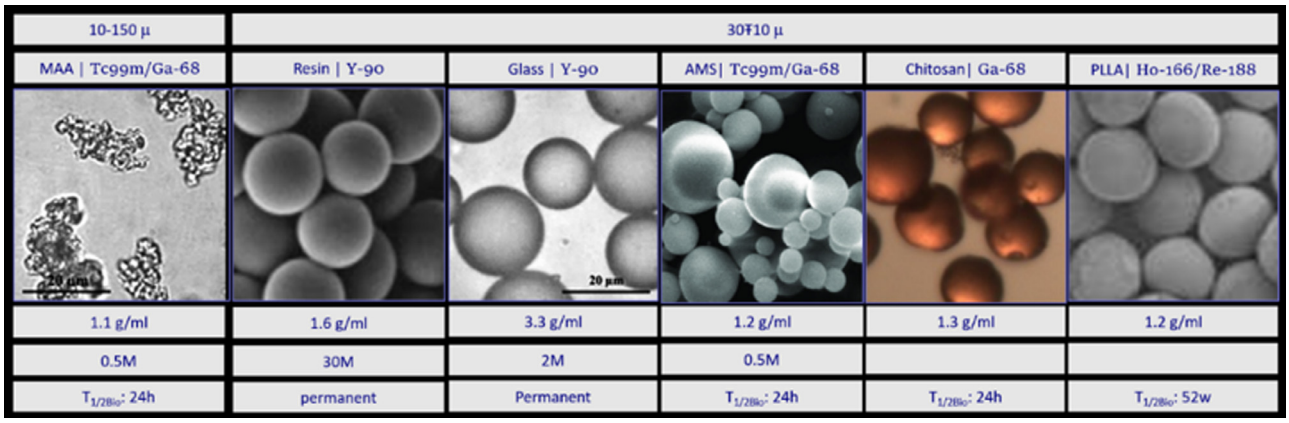

Figure 8 Comparison of microscope images of MAA intended as a surrogate to microspheres used for therapy.

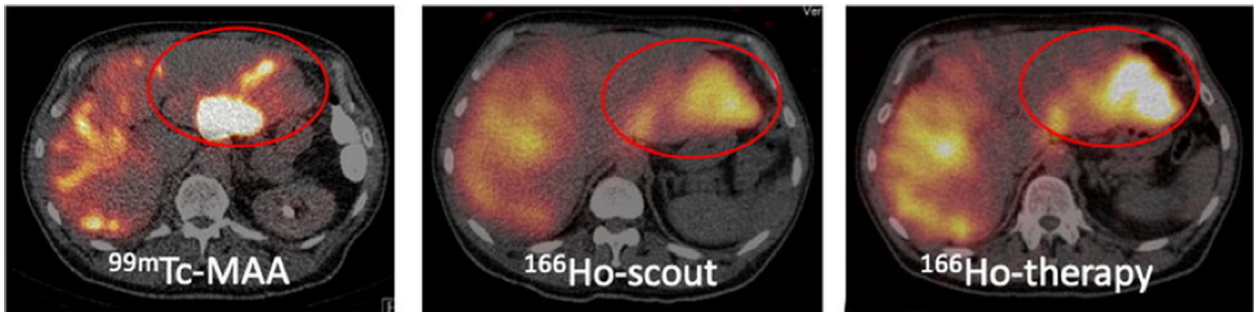

Figure 9 Example of mismatch between Tc-99m-MAA and microspheres. Despite identical catheter positions, there is a remarkable difference in activity distribution between Tc-99m MAA and Ho-166-PLA. A: Tc-99m MAA pre-therapy diagnostic SPECT-CT, B: Ho-166-scout (pre-therapy diagnostic) SPECT/CT, C: Ho-166- post-therapy SPECT/CT.[81]

depression, due to a leak of free Y-90 from the resin microspheres and translocation onto bone and bone marrow radiation exposure is conceivable. This is extremely rare and may only happen with resin but never with glass microspheres since Y-90 is a constituent of the glass microspheres and leach cannot occur. These occurrences are not in the dominion of dosimetry. Safety criteria for both lungs and liver exist. However, these criteria are derived from different foundations, but not through a consistent, uniform theranostic RMT dosimetry data, confirmed with clinical evidence indicating non−toxicity, and comparison with a reliable post-treatment dosimetry. Lung shunt fraction (LSF) is an established index to avoid lung toxicity. A radiation absorbed dose of 30Gy as an MTD comes from the early experience reported with partition model in 1996.[72] There exists a safe radiation absorbed dose limit of 40 Gy based on early generation XRT data published by Ingold et al in 1965.[86] A liver MTD of 120 Gy, specific to the RMT modality, is based on the estimates generated using MIRD, non−compartmental method with Y-90 glass RMT.[87-90] Safety evaluation is also complicated by the preexisting liver disease either due to extensive disease or prior therapeutic interventions. Early reports suggested that the activity of Y-90 Glass microspheres that delivered between 80 Gy and 150 Gy to a lobe of the liver-containing tumor was safe. Patients with significant cirrhosis were treated more conservatively (80-100 Gy), whereas patients without cirrhosis were treated more aggressively (100-150 Gy). A post-therapy dosimetry study using Y-90 SPECT/CT MIRD compartmental model concluded that a Liver dose of 52Gy was associated with 50% possibility of more than grade 2 liver toxicity in patients with HCC.[91] Another post-therapy dosimetry study using Y-90 PET/CT MIRD voxel dosimetry concluded that no toxicity was observed in patients with a liver dose of 54Gy[X].[92] In a more recent study (Dosisphere-01), HCC patients with solitary lesions were randomized for dosimetric method used to determine a liver dose of 120Gy. This study compared the outcomes in groups evaluated using MIRD, non−compartmental method, and theranostic MIRD voxel dosimetry method. The study did not appear to produce meaningful safety data.[93] A review of the most recent consensus and/or guideline manuscripts clearly indicate that there is a definite need for developing a consistent, uniform theranostic RMT dosimetry method.[94,95]

New Generation Radiomicrospheres With Intrensic Theranostic Properties

Pre-clinical research and clinical work continues to overcome the shortcomings of MAA to produce a microsphere with strong theranostic power. Ho-166 PLLA (poly(L-lactic acid) microspheres (QuiremSpheres) were approved in Europe in 2015, awaiting FDA approval in the US. Re-188 PLLA

microspheres are in preclinical investigation phase. They both have gamma emissions suitable for SPECT imaging and have low density favorable rheology.

Non−radioactive holmium-165 (Ho-165) and its acetylacetonate complex (HoAcAc) are incorporated into the poly (L-lactic acid) matrix to form microspheres. Subsequently, the non−radioactive Ho-165-PLLA-MS are made radioactive by neutron activation to form Ho-166-PLLA-MS. Ho-166 decays with a half-life of 27h by emission of β particles with mean energy of 1.8 MeV. At the same time, Ho-166 emits 81 keV γ photons allowing for in vivo imaging by SPECT for theranostic dosimetry calculations. QuiremScout is marketed as a theranostic for QuiremSphere and contains 3 million of the Ho-166 PLLA microspheres, with a total activity of max. 300 MBq (Fig. 9). Ho-166 PLLA microspheres also have paramagnetic properties and can be imaged by MRI.[96,97]

A large body of work was performed by Urs Hafeli for the development of Re-188 PLLA. Uniformly-sized Poly (L-lactic acid) is a biodegradable polyester with a narrow size variation and a similar density to blood were labeled with Re-188.[41,98] Re-188 decays with a half-life of 17 h by emission of β particles with maximum and mean energies of 2.12 and 0.76 MeV, respectively. At the same time, Re-188 emits 155 keV γ photons with an abundance of 15.6%, allowing for in vivo imaging by SPECT for theranostic dosimetry calculations.[41,96,97]

Dose-Effect Relationship and Biologically Effective Dose (BED)

Clinical objective response to RMT and radionuclide therapy in general is dependent on (1) radiation absorbed dose and (2) biological effect produced by the absorbed dose. The latter is mainly an integrated function of cell cycle properties of the target tumor, tissue oxygenation, and the repair rate of the sub-lethal damage.

A Linear-Quadric (LQ) formula has been in use for many decades to quantify response of normal tissue and tumor to external beam radiotherapy. LQ (in various forms) describes the probability of survival (S) of cells following a single radiation dose (D)[99-101]:

$$S = e^{-\alpha D-\beta D^2}$$

The constants α (linear contribution) and β (quadratic contribution) describe the cell's sensitivity to radiation. The ratio α/β (having units of Gy) has been empirically derived for various cell types exposed to various radiation types and energy. Cells with a high α/β ratio experience a relatively constant increase in cell death rate with dose while a low α/β ratio represents greater cell sensitivity with increasing dose.[102] It was suggested that the α term reflects death from "single hit" events while the β term represents "multiple hit" cell death from the effects of different radiation tracks.

"Biologically Effective Dose" (BED) represents the total amount of lethal damage to a particular tissue. BED is derived from the LQ formula.[103,104]

$$BED = nd\left(1+\frac{d}{[\alpha/\beta]}\right)-\frac{\log_e 2(T-T_k)}{(\alpha T_p)}$$

Where "n" in this formula represents the number of fractions in external beam radiation therapy and "d" is the dose in a single fraction. It should be noted that in RMT there is no fractionation. T is the overall time of the therapy (in days). T_p is the cell doubling time. Tumor repopulation starts after day T_k. It should also be noted that the concepts of LQ and BED were developed and applied to external bean radiation in which the radiation exposure is uniform within the tissue. For the case of radionuclide therapy, and radiomicrosphere therapy, the radiation exposure to the cells within the normal and tumor tissue is not uniform, due to the non−uniformity of the vasculature within the tissue. In fact, non−uniform dose is a major concern for RMT since it does not guarantee complete kill of the tumor since the cells within the tumor are not all equally irradiated. Some cells may actually become resistant following exposure to sublethal radiation dose. The non−uniformity problem in radionuclide therapy was first addressed in radioimmunotherapy, generating the concept of equivalent uniform biologically effective dose (EUBED).[105]

The concept of BED was applied to liver directed RMT.[106-110] Unlike fractionated external beam radiation, RMT exposes the cells to the radiation over an extended period of time, with the instantaneous dose decreasing as the radioisotope decays.

$$BED = D\left(1+\frac{DT_{rep}}{(T_{rep}+T_{eff})(\alpha/\beta)}\right)$$

Where T_{eff} is the decay half-life of 90-Y (62.5 h) and T_{rep} is the halftime for cell damage repair (2.5 h for normal tissue and 1.5 h for tumor). The ratio α/β used was typically 2.5 Gy for normal tissue and 10 Gy for tumor. Dose (D) for normal and tumor are obtained from calculating fractional uptake derived from SPECT/CT images of 99mTc-MAA and clinical liver CT assuming a delivered dose of 50 Gy*kg/GBq. At the voxel level, to account for non−uniform distribution if BED can be measured in each voxel (i) of n voxels:

$$EUBED = -\frac{1}{\alpha}\ln\left(\frac{\sum_{i=1}^{n} e^{-\alpha BED_i}}{n_{voxel}}\right)$$

With sufficiently high resolution and sensitivity data dose volume histograms (DVH) and 3-demensional BED distribution are possible.

As stated earlier, absorbed dose, dosimetry concepts are interconnected with biological effect produced by the absorbed dose. The clinical objective responses are intimately dependent on BED and EUBED.

Epilogue

Dosimetric calculations are based on reasonable biologic assumptions and reasonably accurate measurements of the activity distribution. As such, the term "dose estimates" is

preferred. Dosimetry is a computational science. Reproducibility prevails. In a study comparing MIRD compartmental method to MIRD voxel dosimetry, in a HCC patient population, regardless of type of the microspheres, both for tumor, and normal liver dose estimates did not show any significant statistical differences.[111] The results humbly testify that any quantitation is better than no quantitation. Clinical dosimetry applications start from a non−compartmental model, escalate in complexity to a compartmental model, and peak at voxel-based modeling apropos for theranostic dosimetry. The quality of the output of any computational model is only as good as the quality of the input. Dosimetry certainly has an important "Theranostic Value." The "Theranostic Power" refers to accuracy and reproducibility of the dosimetric methodology which ultimately determines the "Theranostic Performance").

References

1. Gulec SA, O'Leary JP: A tribute to a nuclear surgeon - Dr Irving M. Ariel. Arch Surg 142:683-684, 2007
2. Ariel IM: The treatment of primary and metastatic cancer of the liver. Surgery 39:70-91, 1956
3. Ariel IM: The treatment of metastases to the liver with interstitial radioactive isotopes. Surg Gynecol Obstet 110:739-745, 1960
4. Ariel IM: Treatment of inoperable primary pancreatic and liver cancer by intra-arterial administration of radioactive isotopes (Y90 radiating microspheres). Ann Surg 162:267, 1965
5. Ariel IM, Pack GT: Treatment of inoperable cancer of liver by intra-arterial radioactive isotopes and chemotherapy. Cancer 20:793-804, 1967
6. Ariel IM, Pack GT: Treatment of inoperable cancer of the liver by intra arterial radioactive isotopes and chemo. Therapy: 292, 1970.
7. Ariel IM: The treatment of metastatic cancer of the liver from primary cancers of the rectum and colon. Results of different means of therapy. Panminerva Medic 17:405-408, 1975
8. Ariel IM, Padula G: Treatment of symptomatic metastatic cancer to the liver from primary colon and rectal cancer by the intra-arterial administration of chemotherapy and radioactive isotopes. Prog Clin Cancer 7:247-254, 1978
9. Ariel IM, Padula G: The treatment of metastatic cancer to the liver by the intra-hepatic artery administration of chemotherapy and internal irradiation (Y-90 microspheres). Int J Radiat Oncol Biol Phys 6:42, 1980
10. Gray BN: Polymer based radionuclide containing particulate material. Official Gazette of the United States Patent and Trademark Office Patents 2021 https://pubchem.ncbi.nlm.nih.gov/patent/US-11097021-B2
11. Sir-sphere summary of safety and effectiveness data 2021. https://www.accessdata.fda.gov/cdrh_docs/pdf/P990065b.pdf
12. Stribley KV, Gray BN, Chmiel RL, et al: Internal radiotherapy for hepatic metastases .2. the blood-supply to hepatic metastases. J Surg Res 34:25-32, 1983
13. Stribley KV, Gray BN, Chmiel RL, et al: Internal radiotherapy for hepatic metastases .1. the homogeneity of hepatic arterial blood-flow. J Surg Res 34:17-24, 1983
14. Meade VM, Burton MA, Gray BN, et al: Distribution of different sized microspheres in experimental hepatic-tumors. Eur J Cancer Clin Oncol 23:37-41, 1987
15. Burton MA, Gray BN, Jones C, et al: Intraoperative dosimetry of Y-90 in liver-tissue. Nucl Med Biol 16:495-498, 1989
16. Burton MA, Gray BN, Klemp PF, et al: Selective internal radiation-therapy - distribution of radiation in the liver. Eur J Cancer Clin Oncol 25:1487-1491, 1989
17. Gray BN, Burton MA, Kelleher DK, et al: Selective internal radiation (sir) therapy for treatment of liver metastases - measurement of response rate. J Surg Oncol 42:192-196, 1989
18. Archer SG, Gray BN: Vascularization of small liver metastases. Br J Surg 76:545-548, 1989
19. Fox RA, Klemp PFB, Egan G, et al: Dose distribution following selective internal radiation-therapy. Int J Radiat Oncol Biol Phys 21:463-467, 1991
20. Sarfaraz M, Kennedy AS, Cao ZJ, et al: Radiation dose distribution in patients treated with Y-90 microspheres for non-resectable hepatic tumors. Int J Radiat Oncol Biol Phys 51:32-33, 2001
21. Kennedy AS, Van Echo DA, Murthy R, et al: Colorectal (CRC) liver metastases and hepatocellular (HCC) treated with outpatient hepatic artery brachytherapy, therasphere: imaging response and toxicity. Int J Cancer: 226-227, 2002.
22. Mourtzikos K, Lodge MA, Maragh M, et al: Measurement of hepatopulmonary shunt fraction prior to Y-90 microsphere treatment of hepatic malignancy. J Nucl Med 43:317P, 2002
23. Kennedy AS, Van Echo DA, Murthy R, et al: Hepatic artery brachytherapy for neuroendocrine carcinoma. Regulatory peptides 108:32, 2002
24. Sarfaraz M, Kennedy AS, Cao ZJ, et al: Physical aspects of yttrium-90 microsphere therapy for nonresectable hepatic tumors. Medical physics 30:199-203, 2003
25. Sarfaraz M, Kennedy AS, Lodge MA, et al: Radiation absorbed dose distribution in a patient treated with yttrium-90 microspheres for hepatocellular carcinoma. Med Phys 31:2449-2453, 2004
26. Kennedy AS, Nutting C, Coldwell D, et al: Pathologic response and microdosimetry of Y-90 microspheres in man: review of four explanted whole livers. Int J Radiat Oncol Biol Phys 60:1552-1563, 2004
27. Kennedy AS, Coldwell D, Nutting C, et al: Resin Y-90-microsphere brachytherapy for unresectable colorectal liver metastases: modern USA experience. Int J Radiat Oncol Biol Phys 65:412-425, 2006
28. Chauhan N, Bukovcan J, Boucher E, et al: Intra-arterial therasphere yttrium-90 glass microspheres in the treatment of patients with unresectable hepatocellular carcinoma: protocol for the STOP-HCC phase 3 randomized controlled trial. JMIR Res Protoc 7:e11234, 2018
29. Chauhan N, Mulcahy MF, Salem R, et al: TheraSphere yttrium-90 glass microspheres combined with chemotherapy versus chemotherapy alone in second-line treatment of patients with metastatic colorectal carcinoma of the liver: protocol for the EPOCH phase 3 randomized clinical trial. JMIR Res Protoc 8:e11545, 2019
30. Wong CYO, Qing F, Savin M, et al: Reduction of metastatic load to liver after intraarterial hepatic yttrium-90 radioembolization as evaluated by [18F]fluorodeoxyglucose positron emission tomographic imaging. J Vasc Interv Radiol 16:1101-1106, 2005
31. Salem R, Thurston KG: Radioembolization with 90Yttrium microspheres: A state-of-the-art brachytherapy treatment for primary and secondary liver malignancies: part 1: technical and methodologic considerations. J Vasc Interv Radiol 17:1251-1278, 2006
32. Young JY, Rhee TK, Atassi B, et al: Radiation dose limits and liver toxicities resulting from multiple yttrium-90 radioembolization treatments for hepatocellular carcinoma. J Vasc Interv Radiol 18:1375-1382, 2007
33. Jakobs TF, Saleem S, Atassi B, et al: Fibrosis, portal hypertension, and hepatic volume changes induced by intra-arterial radiotherapy with (90)Yttrium microspheres. Dig Dis Sci 53:2556-2563, 2008
34. Kulik LM, Carr BI, Mulcahy MF, et al: Safety and efficacy of Y-90 radiotherapy for hepatocellular carcinoma with and without portal vein thrombosis. Hepatology 47:71-81, 2008
35. Salem R, Padia SA, Lam M, et al: Clinical and dosimetric considerations for Y90: recommendations from an international multidisciplinary working group. Eur J Nucl Med and Molecular Imaging 46:1695-1704, 2019
36. Lewandowski RJ, Salem R: Radioembolisation with personalised dosimetry: improving outcomes for patients with advanced hepatocellular carcinoma. Lancet Gastroenterol Hepatol 6:2-3, 2021

37. Gulec SA, Pennington K, Hall M, et al: Preoperative Y-90 microsphere selective internal radiation treatment for tumor downsizing and future liver remnant recruitment: a novel approach to improving the safety of major hepatic resections. Wld J Surg Oncol 7:6, 2009
38. Amor Coarasa A, Manchanda R, McGoron A, et al: Chitosan microspheres: therapeutic agent for liver-directed radiomicrosphere therapy 2012; 53: 1707.
39. Gulec SA, Pennington K, Wheeler J, et al: Yttrium-90 microsphere-selective internal radiation therapy with chemotherapy (Chemo-SIRT) for colorectal cancer liver metastases an in vivo double-arm-controlled phase ii trial. Am J Clin Oncol -Cancer Clin Trials 36:455-460, 2013
40. Jamre M, Shamsaei M, Erfani M, et al: Preparation and evaluation of Re-188 sulfide colloidal nanoparticles loaded biodegradable poly (L-lactic acid) microspheres for radioembolization therapy. J Labelled Comp Radiopharm 61:586-594, 2018
41. De la Vega Jose Carlos, Esquinas PL, Rodriguez-Rodriguez C, et al: Radioembolization of hepatocellular carcinoma with built-in dosimetry: first in vivo results with uniformly-sized, biodegradable microspheres labeled with re-188. Theranostics 9:868-883, 2019
42. Gulec SA, Suthar R, Barot T: Radiomicrosphere therapy of liver tumors. In: Aktolun C, Goldsmith SJ (eds): Nuclear Medicine Therapy, Springer, 177-198, 2013
43. Gulec A, Fong B: Yttrium-90 microsphere radiomicrosphere therapy of hepatic malignancies. In: Fong Y, Dong JH (eds): HEPATOBILIARY CANCER, USA: Shelton, Connecticut: Medical Publishing House, 2013
44. Gulec SA: Y-90 radiomicrosphere therapy for colorectal cancer liver metastases. Semin Nucl Med 46:126-134, 2016
45. Gulec SA: Y-90 radiomicrosphere therapy: principles and clinical use in colorectal cancer liver metastases. Fong, Gamblin, Lee, editors. Y-90 radiomicrosphere therapy: principles and clinical use in colorectal cancer liver metastases. Cancer Reg Ther: 27-42, 2019
46. Prince JF, van den Bosch Maurice AAJ, Nijsen JFW, et al: Efficacy of radioembolization with Ho-166-microspheres in salvage patients with liver metastases: a phase 2 study. J Nucl Med 59:582-588, 2018
47. QuiremSpheres instructions for use 2021. https://quirem.com/download/LS1101-10_06-IFU-QuiremSpheres-Multi-Language.pdf
48. Basciano CA, Kleinstreuer C, Kennedy AS, et al: Computer modeling of controlled microsphere release and targeting in a representative hepatic artery system. Ann Biomed Eng 38:1862-1879, 2010
49. Kleinstreuer C, Basciano CA, Childress EM, et al: A new catheter for tumor targeting with radioactive microspheres in representative hepatic artery systems. Part I: impact of catheter presence on local blood flow and microsphere delivery. J Biomech Eng 134:051004, 2012
50. Kennedy AS, Clipp R, Christensen D: First-in-human fractal methodology for modeling the hepatic arterial tree and tumor microvasculature for Y-90-microsphere brachytherapy. J Clin Oncol 32, 2014
51. Ackerman NB, Lien WM, Kondi ES, et al: Blood supply of experimental liver metastases .i. distribution of hepatic artery and portal vein blood to small and large tumors. Surgery 66:1067, 1969
52. Lien WM, Ackerman NB: Blood supply of experimental liver metastases .2. a microcirculatory study of normal and tumor vessels of liver with use of perfused silicone rubber. Surgery 68:334, 1970
53. Ackerman NB: Experimental studies on circulatory dynamics of intrahepatic tumor blood-supply. Cancer 29:435, 1972
54. Ackerman NB, Silverman NA, Lien WM: Blood-supply of experimental liver metastases .3. effects of acute ligation of hepatic-artery or portal vein. Surgery 71:636, 1972
55. Ackerman NB, Hechmer PA: Effects of pharmacological agents on the microcirculation of tumors implanted in the liver. Bibl Anat 15:301-303, 1977
56. Ackerman NB, Makohon S: The blood-supply of experimental liver metastases .7. further-studies on increased tumor vascularity caused by epinephrine. Microcirculation Endothelium Lymphatics 1:547-568, 1984
57. Ackerman NB, Jacobs R: The blood-supply of experimental liver metastases .8. increased capillary blood-flow within liver-tumors with administration of epinephrine. Microcirculation Endothelium Lymphatics 2:457-475, 1985
58. Ackerman NB: Experimental studies on the role of the portal circulation in hepatic tumor vascularity. Cancer 58:1653-1657, 1986
59. Stabin M: Nuclear medicine dosimetry. Phys Med Biol 51:R187-R202, 2006
60. Rong X, Ghaly M, Frey EC: Optimization of energy window for Y-90 bremsstrahlung SPECT imaging for detection tasks using the ideal observer with model-mismatch. Medical physics 40:062502, 2013
61. Elschot M, Vermolen BJ, Lam MGEH, et al: Quantitative comparison of PET and bremsstrahlung SPECT for imaging the in vivo yttrium-90 microsphere distribution after liver radioembolization. PLoS ONE 8: e55742, 2013
62. Mikell J, Siman W, Mahvash A, et al: Kernel based dosimetry for 90Y microsphere liver therapy using 90Y bremsstrahlung SPECT/CT. Medical physics 41:438, 2014
63. Debebe SA, Franquiz J, McGoron AJ: 3D dosimetry estimation for selective internal radiation therapy using SPECT/CT images: a phantom study. Med Imag 2015: Phys Med Imag 9412:941234, 2015
64. Nezami N, Kokabi N, Camacho JC, et al: Y-90 radioembolization dosimetry using a simple semi-quantitative method in intrahepatic cholangiocarcinoma: Glass versus resin microspheres. Nucl Med Biol 59:22-28, 2018
65. Debebe SA, Adjouadi M, Gulec SA, et al: 90Y SPECT/CT quantitative study and comparison of uptake with pretreatment 99mTc-MAA SPECT/CT in radiomicrosphere therapy. J Appl Clin Med Phys 20:30-42, 2019
66. Kunnen B, Dietze MMA, Braat Arthur JAT, et al: Feasibility of imaging Y-90 microspheres at diagnostic activity levels for hepatic radioembolization treatment planning. Medical physics 47:1105-1114, 2020
67. Attarwala AA, Molina-Duran F, Buesing K-, et al: Quantitative and qualitative assessment of Yttrium-90 PET/CT imaging (vol 9, e110401, 2014). Plos One 10:e0118423, 2015
68. Takahashi A, Himuro K, Baba S, et al: Comparison of TOF-PET and bremsstrahlung SPECT images of Yttrium-90: a monte carlo simulation study. Asia Oceania J Nucl Med & biology 6:24-31, 2018
69. Osborne DR, Acuff SN, Neveu ML, et al: Feasibility assessment of yttrium-90 liver radioembolization imaging using amplitude-based gated PET/CT. Nucl Med Commun 39:222-227, 2018
70. Duan H, Khalaf MH, Ferri V, et al: High quality imaging and dosimetry for yttrium-90 (Y-90) liver radioembolization using a SiPM-based PET/CT scanner. European J Nucl Med Mol Imag 48:2426-2436, 2021
71. DRAXIMAGE® MAA package insert 2021. https://www.accessdata.fda.gov/drugsatfda_docs/label/2009/017881s010lbl.pdf
72. Ho S, Lau WY, Leung TWT, et al: Partition model for estimating radiation doses from yttrium-90 microspheres in treating hepatic tumours. European J Nucl Med 23:947-952, 1996
73. Ho S, Lau WY, Leung TWT, et al: Clinical evaluation of the partition model for estimating radiation doses from yttrium-90 microspheres in the treatment of hepatic cancer. European J Nucl Med 24:293-298, 1997
74. Amor-Coarasa A, Milera A, Carvajal D, et al: (68)Ga-NOTA-CHSg and (99m)Tc-CHSg labeled microspheres for lung perfusion and liver radiomicrospheres therapy planning. Int J Mol Imaging 2013:279872, 2013
75. Amor-Coarasa A, Milera A, Carvajal D, et al: Lyophilized Kit for the preparation of the PET perfusion agent [(68)Ga]-MAA. Int J Mol Imaging 2014:269365, 2014
76. Bhatt R, Adjouadi M, Goryawala M, et al: An algorithm for PET tumor volume and activity quantification: without specifying camera's point spread function (PSF). Medical physics 39:4187-4202, 2012
77. Goryawala M, Guillen MR, Cabrerizo M, et al: A 3-D liver segmentation method with parallel computing for selective internal radiation therapy. IEEE Trans Inf Technol Biomed 16:62-69, 2012
78. Goryawala M, Gulec S, Bhatt R, et al: A low-interaction automatic 3D liver segmentation method using computed tomography for selective internal radiation therapy. BioMed Res Int 2014:198015, 2014
79. MIRD Pamphlet No 11. 2021. https://s3.amazonaws.com/rdcms-snmmi/files/production/public/MIRD%20Pamphlet%2011.pdf

80. Feller PA, Sodd VJ, Kereiakes JG: Using S tables of mird pamphlet-11. J Nucl Med 18:747, 1977
81. Smits MLJ, Dassen MG, Prince JF, et al: The superior predictive value of Ho-166-scout compared with Tc-99m-macroaggregated albumin prior to Ho-166-microspheres radioembolization in patients with liver metastases. Eur J Nucl Med Mole Imag 47:798-806, 2020
82. Seevinck PR, van de Maat Gerrit H, de Wit TC, et al: Magnetic resonance imaging-based radiation-absorbed dose estimation of Ho-166 microspheres in liver radioembolization. Int J Radiat Oncol Biol Phys 83:E437-E444, 2012
83. Smits MLJ, Nijsen JFW, van den Bosch Maurice AAJ, et al: Holmium-166 radioembolisation in patients with unresectable, chemorefractory liver metastases (HEPAR trial): a phase 1, dose-escalation study. Lancet Oncol 13:1025-1034, 2012
84. Bolch WE, Bouchet LG, Robertson JS, et al: MIRD Comm Soc Nucl Med. MIRD pamphlet No. 17: The dosimetry of nonuniform activity distributions - Radionuclide S values at the voxel level. J Nucl Med 40:11S-36S, 1999
85. Gulec SA, Sztejnberg ML, Siegel JA, et al: Hepatic structural dosimetry in Y-90 microsphere treatment: a Monte Carlo modeling approach based on lobular microanatomy. J Nucl Med 51:301-310, 2010
86. Ingold JA, Reed GB, Kaplan HS, et al: Radiation Hepatitis. Am J Roentgenol Radium Ther Nucl Med 93:200, 1965
87. Salem R, Thurston K: Radioembolization with 90-yttrium microspheres: a state-of-the-art brachytherapy treatment for primary and secondary liver malignancies. Part 1: technical and methodological considerations (vol 17, pg 1251, 2006). J Vasc Interv Radiol 17:1594, 2006
88. Salem R, Thurston KG: Radioembolization with (90)Yttrium microspheres: a state-of-the-art brachytherapy treatment for primary and secondary liver malignancies - Part 2: Special topics. J Vasc Interv Radiol 17:1425-1439, 2006
89. Salem R, Thurston KG: Radioembolization with yttrium-90 microspheres: a state-of-the-art brachytherapy treatment for primary and secondary liver malignancies - Part 3: Comprehensive literature review and future direction. J Vasc Interv Radiol 17:1571-1593, 2006
90. Allimant C, Kafrouni M, Delicque J, et al: Tumor targeting and three-dimensional voxel-based dosimetry to predict tumor response, toxicity, and survival after yttrium-90 resin microsphere radioembolization in hepatocellular carcinoma. J Vasc Interv Radiol 29:1662-1670, 2018
91. Strigari L, Sciuto R, Rea S, et al: Efficacy and toxicity related to treatment of hepatocellular carcinoma with Y-90-SIR spheres: radiobiologic considerations. J Nucl Med 51:1377-1385, 2010
92. Richetta E, Pasquino M, Poli M, et al: PET-CT post therapy dosimetry in radioembolization with resin 90Y microspheres: Comparison with pre-treatment SPECT-CT 99mTc-MAA results. Phys Med 64:16-23, 2019
93. Garin E, Tselikas L, Guiu B, et al: Personalised versus standard dosimetry approach of selective internal radiation therapy in patients with locally advanced hepatocellular carcinoma (DOSISPHERE-01): a randomised, multicentre, open-label phase 2 trial. Lancet Gastroenterol Hepatol 6:17-29, 2021
94. Hong K, Akinwande O, Bodei L, et al: ACR-ABS-ACNM-ASTRO-SIR-SNMMI practice parameter for selective internal radiation therapy or radioembolization for treatment of liver malignancies. Brachytherapy 20:497-511, 2021
95. Levillain H, Bagni O, Deroose CM, et al: International recommendations for personalised selective internal radiation therapy of primary and metastatic liver diseases with yttrium-90 resin microspheres. Euro J Nucl Med Mol Imag 48:1570-1584, 2021
96. van de Maat Gerrit H, Seevinck PR, Elschot M, et al: MRI-based biodistribution assessment of holmium-166 poly(L-lactic acid) microspheres after radioembolisation. Eur Radiol 23:827-835, 2013
97. Seevinck PR, van de Maat Gerrit H, de Wit TC, et al: Magnetic resonance imaging-based radiation-absorbed dose estimation of Ho-166 microspheres in liver radioembolization. Int J Radiat Oncol Biol Phys 83:E437-E444, 2012
98. Jamre M, Shamsaei M, Erfani M, et al: Preparation and evaluation of Re-188 sulfide colloidal nanoparticles loaded biodegradable poly (L-lactic acid) microspheres for radioembolization therapy. J Labelled Comp Radiopharm 61:586-594, 2018
99. Douglas BG, Fowler JF: The effect of multiple small doses of x rays on skin reactions in the mouse and a basic interpretation. Radiat Res 66:401-426, 1976
100. Mclarty JW, Thames HD: Parametric method for estimation of dose-modifying factors - low-dose extrapolation limit. Radiat Res 69:1-15, 1977
101. Dale RG: The application of the linear-quadratic dose-effect equation to fractionated and protracted radiotherapy. Br J Radiol 58:515-528, 1985
102. McMahon SJ: The linear quadratic model: usage, interpretation and challenges. Phys Med Biol 64:01TR01, 2019
103. Fowler JF: The linear-quadratic formula and progress in fractionated radiotherapy. Br J Radiol 62:679-694, 1989
104. Fowler JF: 21 years of biologically effective dose. Br J Radiol 83:554-568, 2010
105. O'Donoghue JA: Implications of nonuniform tumor doses for radioimmunotherapy. J Nucl Med 40:1337-1341, 1999
106. Cremonesi M, Ferrari M, Bartolomei M, et al: Radioembolisation with Y-90-microspheres: dosimetric and radiobiological investigation for multi-cycle treatment. Euro J Nucl Med Mol Imag 35:2088-2096, 2008
107. Ng SC, Lee VH, Law MW, et al: Patient dosimetry for Y-90 selective internal radiation treatment based on Y-90 PET imaging. J Appl Clin Med Phys 14:212-221, 2013
108. Wang T-H, Huang P-I, Hu Y-W, et al: Combined Yttrium-90 microsphere selective internal radiation therapy and external beam radiotherapy in patients with hepatocellular carcinoma: From clinical aspects to dosimetry. PLoS ONE 13:e0190098, 2018
109. Dewaraja YK, Devasia T, Kaza RK, et al: Prediction of tumor control in Y-90 radioembolization by logit models with PET/CT-based dose metrics. J Nucl Med 61:104-111, 2020
110. Willowson KP, Eslick EM, Bailey DL: Individualised dosimetry and safety of SIRT for intrahepatic cholangiocarcinoma. Ejnmmi Physics 8:65, 2021
111. Gallio E, Richetta E, Finessi M, et al: Calculation of tumour and normal tissue biological effective dose in Y-90 liver radioembolization with different dosimetric methods. Physica Medica-Eur J Med Phys 32:1738-1744, 2016